

## Chapter 4

### **CHRONOLOGY AND AGE MODEL OF THE CORES**

The chronology of the sediment cores is vital component to study the timeframe of initiation, continuation and changes of geological parameters over a period of time. It facilitates to constrain the scale and duration of the various palaeo-events in the sedimentary basin. There are various methods which are applied to arrive at the chronology which depends on the type of area or material one is dealing with. The recently developed method of AMS radiocarbon dating has enabled to date the event of less than 50,000 calendric years with precise error limit. Other isotopes that have been analyzed using AMS include  $^{10}\text{Be}$ ,  $^{26}\text{Al}$ ,  $^{36}\text{Cl}$ ,  $^{41}\text{Ca}$ , and  $^{129}\text{I}$  (Schoute et al., 1981). The research applications of these isotopes are much the same as for  $^{14}\text{C}$  but are useful for studying processes of time scales greater than the limit of  $^{14}\text{C}$  dating. Some of the dating methods like OSL (optically stimulated luminescence) are also reliable for dating the geological materials and soft sediments (Andree et al., 1986). There are few limitations of the dating tools like AMS (Accelerated Mass Spectroscopy) where due to the small sample size, control of contaminants is a difficult task. Rigorous pre-treatment is needed to make sure that the contaminants have been eliminated and will not lead to substantial errors during the carbon dating process (Schoute et al., 1981). Keeping in view of this limitation it is necessary to make samples contamination free and the process should be carried out in a closed environment.

#### **THE DHORDO CORE AND THE BERADA CORE**

The hyper-saline flat terrain of the Great Rann of Kachchh (GRK) basin comprises sediment deposits of Quaternary age underlain by Tertiary and Mesozoic rocks (Biswas, 1974; Merh, 2005). Owing to the flat terrain of the basin and consequent severe paucity of Quaternary sediment exposures, the use of subsurface sediments is inevitable for reconstructing the geological evolution of the GRK basin. In view of this, two long sediments were raised from the central part of the basin (Dhordo core) and the southern marginal part of the basin in Banni plain (Berada core) which form the first ever cores of Quaternary sediments obtained from GRK (Maurya et al., 2013). The cores are preserved in the Department of Geology, The M. S. University of Baroda, Vadodara sub-zero temperature conditions. The location of the cores is shown in Figure 2.1. Both the cores were sampled at 2 cm interval. The cores mainly comprise fine-grained sediments with

~80% dominance of silt (Maurya et al., 2013; Kumar et al., 2021). Due to its fine-grained sediment nature initially, stressed environmental conditions and silt to fine sand size (Maurya et al., 2013; Khonde et al., 2017a), it was not found feasible to collect foraminifera shells for dating purposes. Moreover, due to fewer presence of Quartz mineral throughout the core OSL dating too was not attempted. However, few AMS radiocarbon dates that include both organic and inorganic carbon, were available on the cores.

Three dates from the Dhordo core and three dates from the Berada core were published by Maurya et al. (2013) and Khonde et al. (2017a, b). In the present study, additional AMS radiocarbon chronology was attempted. The chronological studies in the present attempt was focussed on both on organic and inorganic carbon dating. A total of 30 dates were obtained using organic carbon and 8 data were obtained using inorganic carbon (Kumar et al., 2021). The description below provides details of the chronological studies carried out the in the present study. This followed by the revised age model of the cores based on new inorganic carbon dates and inorganic carbon dates available previously. The age model is based on inorganic carbon dates only as there are uncertainties involved in organic carbon dating as discussed in the later sections.

### **AMS RADIOCARBON DATING OF THE CORES**

Carbon exists in the most part in the isotope C-12, but has a radioactive isotope, C-14, with a half-life of 5570 years (Fowler et al., 1986a, b; Lowe et al. 1988; Vogel et al. 1989). All terrestrial organisms use carbon dioxide present in the atmosphere which act as a source of carbon, thus there is a constant conversation of C-14 with the atmosphere. After the organism dies, the exchange is stopped, and the C-14/C-12 starts disintegrating with the radioactive decay of the C-14 present in the dead organism. Thus, the amount of C-14 present in the sample can give us an estimate of its age. The raw or the bulk samples which is usually used for the organic carbon dating includes all the biologically produced by-products as well as the chemically produced organic products. It includes the leaf and the rootlet tissues.

To minimize the amount of new carbon in the organic sample, the sample must be liberated from coarse and fresh organic material, such as leaf and root tissue. Free carbonates in the sample are eliminated by treatment with hydrochloric acid (HCl). The

remaining material is then dried and burned to CO<sub>2</sub>, and the activity can then be measured by gas proportional counters or by liquid scintillation spectrometers.

The requirement of the sample for the organic carbon dating has its advantage as it does not require any material which is to be separated at the time of collection of the sample. The method eliminates the need of a precise material need to be extracted from the samples at the time of dating (Deevey et al. 1954). Moreover, it is time efficient to collect the sample in its raw form and can be directly taken to the laboratories for the pre-treatments.

Radiocarbon dating of organic sample has always been a tricky problem. Since organic matter is continually being introduced into the sample, the measured age of organic matter has always tended to underestimate the true age of the sample. One of the main problems with this method of organic radiocarbon dating is the presence of a steady state, beyond which <sup>14</sup>C dating will yield no useful information regarding the age of the sample (Teunissen, 1986). Historically, a solution has been to separate the portion of the sample that has a greater age than the remaining fractions and use it to calculate estimate the sample age, but recently more advanced methods of organic carbon dating have appeared, which give better estimations. Using the entire sample and measuring its radioactivity amounts and considering the whole sample to be of the particular age, which involves the fact that the organic material is continually added to the sample. This thus provides only a higher bound on the age of the sample.

### **Organic carbon dating of the cores**

The samples were collected from both cores i.e., Dhordo and Berada cores for the organic carbon dating. To make sure for its organic abundance the samples were collected from the previously marked position from the core during the core examination. To avoid repetition of the of the samples those depths were skipped where the samples were already taken for the inorganic dating. A total of 30 bulk sediment samples from both cores were dated at the IUAC (Inter University Accelerator Centre), New Delhi during the present study (Table 4.1). Three dates on organic material were published earlier (Table 4.2) by Khonde et al. (2017a, b) which were dated from NSF Arizona AMS facility (The University of Arizona, USA). Calibration of the radiocarbon ages to calendar years before present of the 30 samples dated at IUAC in the present study, was completed using the calibration data set by (Reimer et al., 2009). The reservoir effect correction values were

considered from (Dutta et al., 2006). Table 4.1 shows list of the material and other details of the dates from both the cores dated at IUAC New Delhi.

**Table 4.1** AMS Radiocarbon ages (organic carbon) from both the cores (Dhordo and Berada) processed at the IUAC (Inter University Accelerator Centre, New Delhi).

S. No.	Sample Name	Lab ID	pMC value	Radiocarbon Age (yrs B.P.)	Cal. Age (yrs B.P.)	Depth (cm)
1.	DH-1-2	IUACD #17C763	24.453±0.179	11313±58	<b>13166</b>	4
2.	DH-1-4	IUACD #17C764	58.592±0.347	4294±47	<b>4863</b>	8
3.	DH-1-9	IUACD #17C765	20.261±0.152	12824±60	<b>15286</b>	18
4.	DH-3-24	IUACD #17C766	6.815±0.075	21577±89	<b>25865</b>	268
5.	DH-5-21	IUACD #17C767	21.009±0.157	12533±60	<b>14817</b>	500
6.	DH-6-81	IUACD #17C768	16.591±0.131	14429±63	<b>17587</b>	802
7.	DH-7-3	IUACD #17C769	19.277±0.150	13224±62	<b>15896</b>	1000
8.	DH-8-88	IUACD #17C770	8.397±0.094	19899±90	<b>23948</b>	1412
9.	DH-10-91	IUACD #17C771	13.448±0.118	16116±70	<b>19449</b>	1908
10.	DH-12-49	IUACD #17C772	15.515±0.130	14968±67	<b>18191</b>	2358
11.	DH-14-33	IUACD #17C773	12.534±0.115	16682±74	<b>20128</b>	2726
12.	DH-16-132	IUACD #17C774	11.780±0.118	17180±81	<b>20722</b>	3554
13.	DH-18-91	IUACD #17C775	10.271±0.113	18282±88	<b>22151</b>	4058
14.	DH-21-118	IUACD #17C776	9.559±0.098	18859±82	<b>22715</b>	5062
15.	DH-23-64	IUACD #17C777	7.929±0.085	20361±86	<b>24450</b>	5560
16.	DH-24-29	IUACD #17C778	7.663±0.085	20635±89	<b>24853</b>	5860
17.	BRD-1-1	IUACD #17C779	42.021±0.228	6964±43	<b>7795</b>	2
18.	BRD-1-41	IUACD #17C780	19.986±0.161	12934±65	<b>15458</b>	82
19.	BRD-1-44	IUACD #17C781	15.558±0.126	14945±65	<b>18165</b>	88
20.	BRD-3-38	IUACD #17C782	8.964±0.0895	19374±80	<b>23327</b>	300
21.	BRD-4-70	IUACD #17C783	17.967±0.137	13789±61	<b>16677</b>	486
22.	BRD-5-103	IUACD #17C784	25.224±0.180	11064±57	<b>12928</b>	788
23.	BRD-6-36	IUACD	19.643±0.150	13073±61	<b>15672</b>	988

		#17C785				
24.	BRD-6-136	IUACD #17C786	13.797±0.116	15911±67	<b>19182</b>	1188
25.	BRD-7-131	IUACD #17C787	21.587±0.157	12315±58	<b>14283</b>	1488
26.	BRD-9-80	IUACD #17C788	17.012±0.137	14228±65	<b>17325</b>	1988
27.	BRD-10-61	IUACD #17C789	10.094±0.101	18421±80	<b>22308</b>	2290
28.	BRD-12-61	IUACD #17C790	27.447±0.189	10385±55	<b>12256</b>	2988
29.	BRD-13-128	IUACD #17C791	12.487±0.112	16712±72	<b>20163</b>	3464
30.	BRD-16-18	IUACD #17C792R	8.800±0.141	19523±130	<b>23520</b>	4000

**Table 4.2** Previously available AMS radiocarbon ages from both the cores (Dhordo and Berada) published by Khonde et al. (2017a, b). The samples were processed at The University of Arizona, USA.

S. No.	Sample Name	Lab ID	pMC value	Radiocarbon Age (Kyr)	Cab. Age (Kyr)	Depth (cm)
1.	DH	DHR-2	0.1801 ± 0.0016	13,772 ± 73	16,340 ± 79	4500
2.	DH	DHR-3	0.1522 ± 0.0015	15,123 ± 81	17,700 ± 86	6013
3.	BRD	BRD-3	0.3250 ± 0.0021	9029 ± 53	9515 ± 61	3888

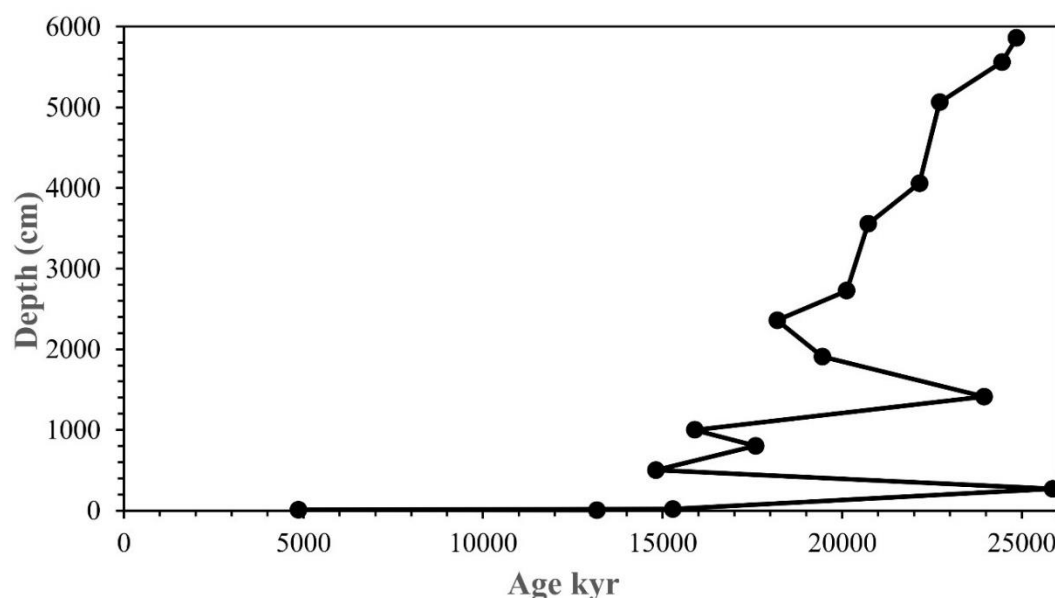


**Figure 4.1** Graphical representation of the all the organic carbon ages from Dhordo core processed at IUAC (Inter University Accelerator Centre, New Delhi). Note the reversal and overestimation of the ages obtained.

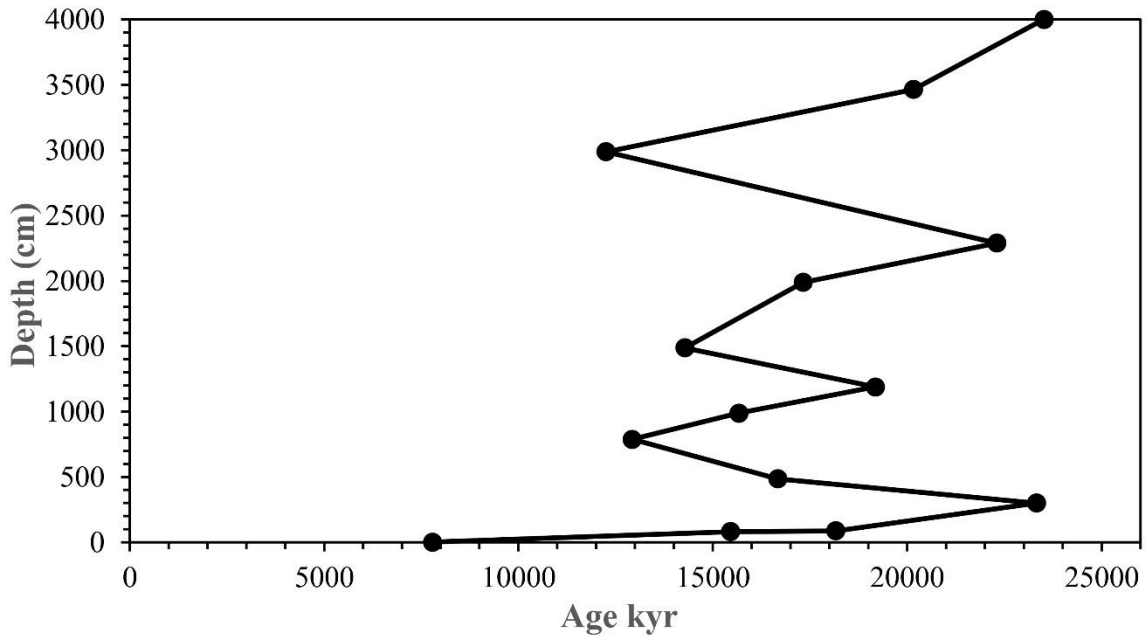


**Figure 4.2** Graphical representation of the all the organic carbon ages from Berada core processed at IUAC (Inter University Accelerator Centre, New Delhi). Note the reversal and overestimation of the ages obtained.

The graphical representation of Age vs depth model using AMS organic carbon dates of both the cores (included in Table 4.1) is shown in Figure 4.1 (Dhordo core) and Figure 4.2 (Berada core). As seen in Figure 4.1 and 4.2 reverse ages of organic carbon dates are obtained. The reverse ages are obtained at the depths of 0.4 m, 14.12 m, 19.19 m in Dhordo and at 3 m, 4.8 m and 11.8 m in berada. Some of the ages also shows over estimation of ages where it reaches as high as 25,854 kyr at the depth of 2.6 m in Dhordo core and up to 23,530 kyr at the depth of 40 m in Berada core. The over estimation and reversed ages are particularly limited to the organic carbon dating in the Great Rann of Kachchh (GRK). Although this problems with the organic carbon are not unique for this basinas it is widely faced by any researchers working in the areas around the northern Arabian sea (Arie et al., 1992). Mook and van de Plassche (1986) have discussed intrinsic geochemical uncertainties as well as incidental difficulties due to botanical and/or mechanical contamination, which may be especially relevant to organic lake sediments. Another effect for overage of sediments is mechanical contamination which may result from various kinds of bioturbation after formation of the deposit. This can be expected particularly in oxidized material (Mook & van de Plassche 1986). The hard water effect is also one of the prime reasons for the contamination of samples where it is probably caused by siderite (P. Cleveringa, 1991).

Few researchers reported the contamination and the aging effect due to the fluvial processes which results not only in an admixture of siliciclastic material, but also in the deposition of reworked, fine-grained organic debris (Schoute et al., 1981; Schoute, Mook and Streurman 1983; Schoute, 1984; Torbjorn e. tornqvist, 1992). The shallow condition of deposition in GRK could also be one of the reasons for the aging affect on the samples. This supposition is also based on the fact that the basin was long under shallowing effect and the sediments deposited in a shallow basin, stagnant water, where there was probably a rapid mixing of CO<sub>2</sub> between water and atmosphere. The surrounding exposure effect is also one among many effects resulting in aging of the samples. The exposed section around the GRK composed of Mesozoic and Tertiary rocks. The contamination from the exposed limestone section of older age around GRK plays a vital role in aging effect of the organic samples. GRK receives sediment from the surroundings through different mediums such as aeolian and fluvial deposit from the west.

### **Inorganic dating of the cores**

The ability to date samples containing 1 mg C has made possible oceanographic research at high resolution. In addition, small sample sizes have allowed much simpler, less expensive collection of small seawater samples and greater selectivity of sample components to analyze. For example, one may select specific seawater chemical components for analysis and select other than the abundant bulk carbonate from a sediment to date. Radiocarbon analyses of dissolved inorganic carbon (DIC) from surface and subsurface ocean have typically required 200-300l of seawater for conventional measurements of sufficient precision, with even larger samples needed for samples of dissolved organic carbon (DOC). Dissolved inorganic carbon  $\delta^{14}C$  analyses are considered to determine the residence time of dissolved CO<sub>2</sub> in respect to different water masses. Bomb-produced  $^{14}C$  is used as a tracer in the waters above (and now, below) the thermocline. From DIC measurements, rate constants for the mixing of water masses and eddy-diffusion coefficients applicable within masses may be estimated using models (Lister et al., 1984; Andree et al., 1986; MacDonald et. al., 1987; Nelson et al., 1988; Ammann & Lotter, 1989; Cwynarand Watts, 1989; van Geelet al., 1989; Vogel et al., 1989; Peteet et al., 1990). Measurements of dissolved organic carbon, which includes multiple origins such as dissolution of organic matter from phyto- and zooplankton, bacteria, and riverine sources, have been widely used to determine the overall time of

DOC in the deep sea and also to determine the depth of penetration of bomb-produced DOC  $^{14}\text{C}$ .

The measurement of  $^{14}\text{C}$  is complicated by the presence of the isobar  $^{14}\text{N}$  and the molecules  $^{12}\text{CH}_2$  and  $^{13}\text{CH}$ ,  $^{14}\text{N}$  comprises 78% of the atmosphere and may be found even in high vacuum systems at levels which lies much higher than that of  $^{14}\text{C}$ . An AMS instrument eliminates almost all the  $^{14}\text{N}$  before it can proceed through the instrument, due to the fact the nitrogen does not form negative ions. The molecules are eliminated inside the accelerator, which allows good mass resolution both before and especially after the atoms pass through accelerator, moreover it allows simple separation in the final detector of small amounts of  $^{14}\text{N}$ ,  $^{13}\text{C}$ , and  $^{12}\text{C}$  from the  $^{14}\text{C}$  ions of interest (MacDonald et al. 1987). In contrast to decay counting, nearly none of the background level comes from the instrument; most of the background measured is  $^{14}\text{C}$  from contaminants entrained in the sample during its chemical processing. In this laboratory, if we assume that this 'contamination' has the activity of current atmospheric  $\text{CO}_2$ , the  $^{14}\text{C}/^{13}\text{C}$  ratio from a 1 mg sample fabricated from dead material is 0.4 % of the  $^{14}\text{C}/^{13}\text{C}$  ratio obtained from material containing the contemporary atmospheric concentration of  $^{14}\text{C}$  (Shotton 1972; Andree et al. 1986).

The macro fossils are available in sufficient quantities, which is usually the case in organic deposits, are probably the most practical elements in terms of sample preparation time. The macro fossils are likely to yield accurate dating results, provided that they have been formed and deposited in situ. If macrofossils are allogenic, it is essential that they have not been eroded from older geological strata or deposition. As mentioned earlier, the greatest advantage of AMS is the sample size requirement: samples containing 1 mg of carbon after any necessary cleaning or chemical treatment are routinely analyzed by AMS labs to a precision of more or less 50 years or better for samples weighing much less than 5 kg. The original sample size will, of course, depend on the material and its carbon content. The cost expenses of the dating are very high and requires high precision laboratories. The error limit is in the prescribed limit only when the contamination is eliminated very carefully and precisely.

The samples were collected from both cores i.e. Dhordo and Berada for the inorganic dating. To make sure for its inorganic abundance the samples were collected from the previously marked position from the core during the core examination. Due to lack or scarcity of shell from the cores 10 mg of foraminifera was collected for the dating.

The samples were selected based on grain size data generated. The depths having high dominance of sand were selected for the foraminifera collection. Few samples with the presence of broken shell were also collected for the inorganic dating. To avoid repetition of the of the samples those depths were skipped where the samples were already taken for the organic dating. Total of 11 inorganic dates were obtained at following AMS facility: -

During the present study, inorganic AMS dating of four samples were carried out at the WHOI (Woods Hole Oceanography Institute, USA), whereas 4 inorganic samples were dated at AMS facility of PRL (Physical Research Laboratory, Ahmedabad). These are in addition to the three inorganic AMS dates were previously published by Khonde et al. (2017a, b) which were analysed at the NSF Arizona AMS facility (The University of Arizona, USA) Calibration of the radiocarbon dates to calendar years before present was completed using the calibration data set by (Reimer et al., 2009). The reservoir effect correction values were considered from (Dutta et al., 2006). (Table 4.3) shows list of the material and other details of the dates from both the cores dated from various institute mentioned above.

**Table 4.3** Radiocarbon ages from both the cores (Dhordo and Berada) processed at The University of Arizona, USA (after Khonde et al., 2017a, b). Sample material used were shell of macrofossils acquired from both the cores.

S. No.	Sample Name	Lab ID	pMC value	Radiocarbon Age (ysr)	Cab. Age (yrs B.P.)	Depth (cm)
1	DH	DHR-1	0.4369 ± 0.0025	6652 ± 45	6985 ± 54	2578
2	BRD	BRD-4	0.4259 ± 0.0025	6856 ± 45	7235 ± 54	1920
3	BRD	BRD-5	0.3405 ± 0.0022	8654 ± 51	8491 ± 59	3278

**Table 4.4** Radiocarbon ages from both the cores (Dhordo and Berada) obtained in the present study and processed at WHOI (Woods Hole Oceanography Institute, USA) and PRL (Physical Research Laboratory, Ahmedabad). Samples used were foraminifera and broken shells collected at the various depths from the cores.

S. No	Sample Name	Lab ID	pMC value	Radiocarbon Age (yrs)	Cab. Age (yrs B.P.)	Depth (cm)
1	1 (DHR)	WHOI -1	0.6064±0.0015	4,020 ± 20	3750 ± 35	550
2	2 (DHR)	WHOI -2	0.3188±0.0015	9,180 ± 40	8926 ± 93	3845
3	3 (DHR)	WHOI -3	0.3020±0.0015	9,620 ± 40	10190± 40	4992
4	4 (DHR)	WHOI -4	0.3044±0.0016	9,560 ± 40	10232± 59	5992
6	1 (BRD)	BRD/AMS /PRL/1	0.2250 ± 0.1021	5285 ± 202	5485±6003	580
7	2 (BRD)	BRD/AMS /PRL/2	0.4750 ± 0.6021	6417 ± 45	6946±7152	1160

8	3 (BRD)	BRD/AMS /PRL/3	0.4150 ± 0.3221	6564 ± 206	6959±7417	1550
9	4 (BRD)	BRD/AMS /PRL/3	0.3250 ± 0.1121	9207 ± 142	9881-10338	3910

#### AGE MODEL OF THE DHORDO CORE

As a result of the new 14C AMS chronology carried out in the present study a revised age model of the Dhordo and Berada cores is adopted. While the chronology of the Dhordo core is completely revised, the resolution of the Berada core is considerably enhanced. The revised age model of the cores has been possible because of the inorganic dates generated in the present study which is based on the materials like foraminifera shells, Bivalve shell, and few broken shells. Although one of the date form the berada core at the depth of 38.88 m is based on organic was accepted for the new age model as it was in alignment with other ages acquired from the inorganic samples. Our age model has helped to eliminate the long and controversial debate about the use of organic carbon dates which have been earlier proven for its overestimation in terms of age obtained.

The Dhordo core is ~ 60 m long and is noted for its largely fin grained nature of the sediments (Maurya et al., 2013). As mentioned earlier, the core is obtained from the central part of the GRK basin. The chronological data used for reconstruction of the age model of the Dhordo core is given in Table 4.5.

**Table 4.5** AMS radiocarbon ages of Dhordo core used for reconstructing the age model. [#-present study; \*-after Khonde et al., (2017a b)].

S. No.	Sample Name	Material dated	Laboratory Name	Lab ID	pMC value	Radiocarbon Age (yrs)	Cab. Age (yrs B.P.)	Depth (cm)
1	1 (DHR)	Foraminifera shells	WHOI, USA	WHO I-1	0.6064 ± 0.0015	4,020 ± 20	3750 ± 35	550#
2	2 (DHR)	Bivalve shell	NSF, Arizona	DHR-1	0.4369 ± 0.0025	6652 ± 45	6985 ± 54	2578*
3	3 (DHR)	Foraminifera shell	WHOI, USA	WHO I-2	0.3188 ± 0.0015	9,180 ± 40	8926 ± 93	3845#
4	4 (DHR)	Foraminifera shell	WHOI, USA	WHO I-3	0.3020 ± 0.0015	9,620 ± 40	10190 ± 40	4992#
5	5 (DHR)	Foraminifera shell	WHOI, USA	WHO I-4	0.3044 ± 0.0016	9,560 ± 40	10232 ± 59	5992#

The new age model of the Dhordo core is reconstructed using Bayesian age-depth model, where the thickness of the samples is taken into consideration along with the depth and calibrated age (Figure 4.3). There are few advantages of using new technique for calculation of sedimentation rate where the model is automatically corrected for the top and bottom most part of the core. It provides an even distribution for the closely spaced dates from the core. The error limit is less than 5 percent for this age model software which is widely used for the oceanographic sediments age model. The following model is applied for this study to acquire the age model of the core. The sedimentation rate is calculated for the Dhordo core based on the radiocarbon dates (Table 4.5). The sedimentation curve of the Dhordo core suggests the core experienced highest sedimentation during Greenlandian age/Early and Late-Holocene stage. The Dhordo core experienced decreased sedimentation rate during Northgrippian age/ Mid- Holocene which marks the slow and fluctuating sea level change. The lowest sedimentation from the core is noted from the Meghalayan Stage/ Late Holocene where it dips to 0.14 cm/year marking the regression phase of the core (Figure 4.3).

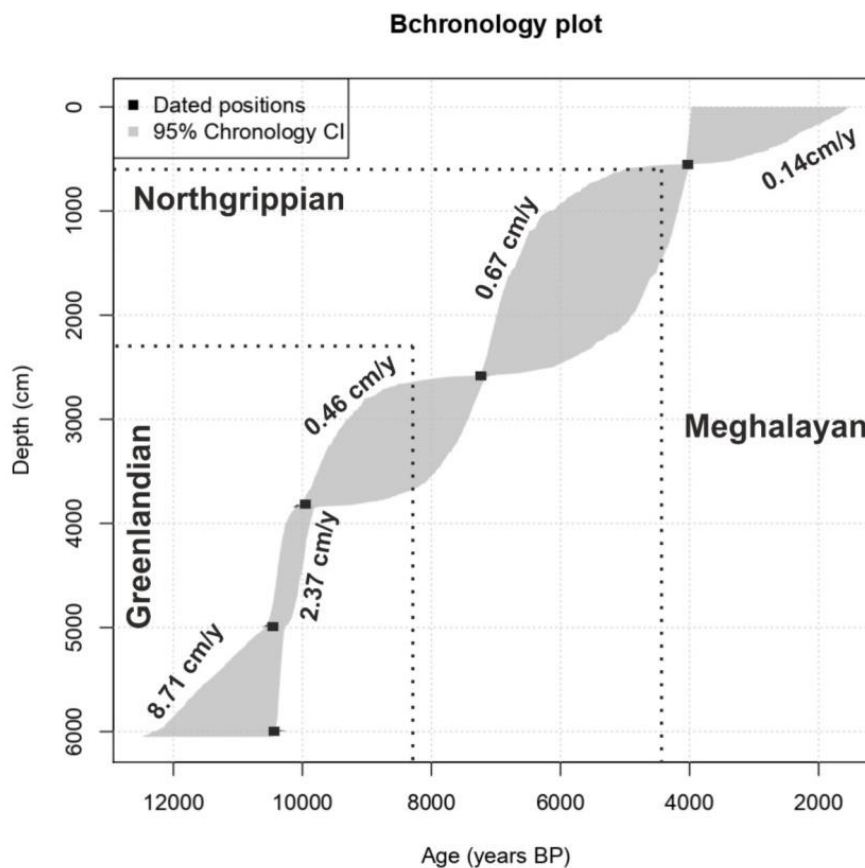


**Figure 4.3** Age model of the Dhordo core reconstruction using the Bayesian age-depth model. Note the high rates of sedimentation throughout the core, especially during the Greenlandian Stage.

In general, the entire length of the Dhordo core is divisible into three divisions as described below.

### **Greenlandian Stage - Early and Late-Holocene**

The age model reconstructed for the Dhordo core in the present study (Figure 4.3) shows rapid deposition and huge accumulation of sediments during the Greenlandian Stage. The sedimentation rate of 8.71 cm/ y is highest from the entire core (Figure 4.3). The huge pile of the sediments broadly correlates with the rapid sea level rise after the Last Glacial Maximum (Hori and Saito, 2007; Tamura et al., 2009). This phenomenon is noted from the other land-marine interaction settings as well. The major delta initiation with unusually high sedimentation rates has also been reported globally during this period as well (ref). Detailed analyses of sediment cores of Asian deltas have provided evidence for the delta initiation in relation to a sea level standstill or a decelerated sea-level rise at around 8.0 calkyr BP, this was followed by a rapid rise in sea level during the period of 9.0–8.2 calkyr BP (e.g., Bird et al., 2007; Hori and Saito, 2007; Tamura et al., 2009; Bird et al., 2010; Nguyen et al., 2010; Li et al., 2012).

The sedimentation rate of the core decreases to 2.41 cm/y from its peak which shows the transition towards the standstill which may have been established in the central part of the basin (Figure 4.3). The decrease in the sedimentary rate points towards the steady and constant sediment accumulation in the basin. Although the sedimentation rate still marks the second highest rate of sedimentation from the entire core. The drastic decrease in the sedimentation rate from 2.14 cm/y to 0.46 cm is noted towards the end of the Greenlandian Stage. The response of the decrease sedimentation rate is in synchronous with the decreased pace of the global sea level. The global sea level shows a constant decrease/standstill in the rise of the sea level towards the end of the Greenlandian Stage. The western continental margin sea level curve also shows decrease in the sea level rise (Rao and Wagle, 1997, Juyal et al., 2006; Tyagi et al., 2012).

### **Northgrippian Stage - Middle Holocene**

The Dhordo core shows slight increase in the sedimentation rate during the Northgrippian Stage -mid-Holocene period where it reaches to 0.67 cm/year from 0.46 cm/ year (Figure 4.3). The slight increase in the sedimentation rate marks the maximum level of the sea and/or slight change in the sea levels due to local factors (Hashimi et al.,

1999). Higher sea level stand during this period therefore may trigger the river channel retreat and finer sediment flux may dominate in the marginal marine basins.

### Meghalayan Stage - Late Holocene

The lowest sedimentation rate is noted during the Meghalayan Stage- Late Holocene period where it reaches to 0.14 cm / year from 0.67 cm/year (Figure 4.3). The period marks the lowest sediment deposit in the core which could be in response to the withdrawal of the sea. The regression period was established during this period and the withdrawal of the sea was completely established from the area (Maurya et al., 2013; Khonde, 2014). This period marks regression phase in the GRK central basin, and the central basin is presently marked in supra tidal conditions. The region was completely exposed at the end of this period. The period records for the drying up of basin which is well supported with the decreased in the sedimentation rate to 0.14 cm/year.

**Table 4.6** Radiocarbon age of Berada core used for the age model in this study. Note that the ages marked with \* are previously published dates by Khonde et al., (2017a b). Ages with # marks are generated during the present study.

S. No	Sample Name	Material dated	Laboratory Name	Lab ID	pMC value	Radio-carbon Age (yrs)	Cal. Age (yrs B.P.)	Depth (cm)
1	BRD/AMS /PRL/1	Broken shell	PRL, Ahmedabad	AURIS-04302	0.2250 ± 0.1021	5285 ± 202	5485±6003	580#
2	BRD/AMS /PRL/2	Broken shell	PRL, Ahmedabad	AURIS-04303	0.4750 ± 0.6021	6417 ± 45	6946±7152	1160 #
3	BRD/AMS /PRL/3	Foraminifera + broken shell	PRL, Ahmedabad	AURIS-04304	0.4150 ± 0.3221	6564 ± 206	6959±7417	1550 #
4	BRD (1)	Bivalve shell	NSF, Arizona	BRD - 1	0.4259 ± 0.0025	6856 ± 45	7235 ± 54	1920 *
5	BRD (2)	Gastropod shell	NSF, Arizona	BRD - 2	0.3405 ± 0.0022	8654 ± 51	8491 ± 59	3238 *
6	BRD (3)	Raw sediments	NSF, Arizona	BRD - 3	0.3250 ± 0.0021	9029 ± 53	9515 ± 61	3888 *
7	BRD/AMS /PRL/4	Foraminifera shell + broken shell	PRL, Ahmedabad	AURIS-04305	0.3250 ± 0.1121	9207 ± 142	9881-10338	3910 #

## AGE MODEL OF THE BERADA CORE

The Banni plain present on the southern flank of the GRK basin is surrounded by KMF (Kachchh Mainland Fault) on its south and by Thar desert on its east. The Berada core is recovered from the Banni plain represent the changes of the GRK basin from the hinterlands where the ephemeral rivers contributed sediments seasonally owing to the hyper arid climate. Based on radiocarbon dating, it appears that the sedimentation was initiated at the southern margin of GRK from the Greenlandian Stage. Presence of fluvial sediments at the bottom most part of the core points towards the transgression of the sea in this part of the GRK. To establish the depositional conditions and the palaeoenvironmental controls on the sediment accumulation, the age model based on the radiocarbon dating was taken into consideration (Table 4.6).

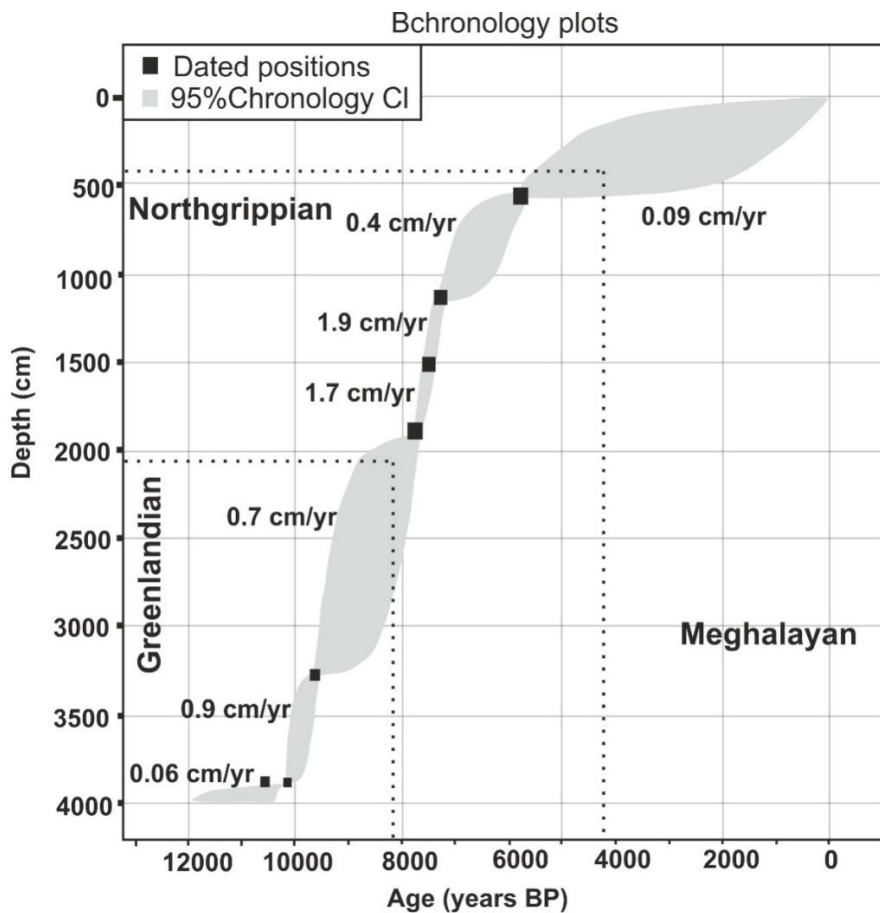


**Figure 4.4** Berada age depth model calculated using Bayesian age-depth model. The graphical representation of the inorganic samples dated at various facilities.

### Greenlandian Stage /Lower and Early Holocene

The sedimentation rate shows very high rate which in agreement with the other land marine settings where the chronological data suggests the increased in sedimentation

rate in the Greenlandian Stage (Figure 4.4). The response of the Banni core is in conformance with the global sea level where a jump in the sedimentation rate could be noted in the Greenlandian Stage (Fairbanks 1989). This rapid rising sea-level was continued further with high sedimentation rate at the Berada core site which is in contrast with the normal estuarine sedimentation. Higher sea level stand during this period therefore may trigger the river channels retreat and finer sediment flux may dominate in the marginal marine basins. This is characterised by sedimentary structures (Alexander et al., 1991; Avramidis et al. 2013). The decrease in the sedimentation from 0.9 cm/year to 0.7 cm/year is noted where the core shifts towards comparatively low sedimentation rate. The core maintains the pace with the rising sea level and continues to show transgression in the Banni plain. This may trigger the formation of estuarine in the Banni plain.

### **Northgrippian Stage/ Mid- Holocene Stage**

The mid Holocene marks the increased sedimentation rate from 0.7 cm/year to 1.7 cm/year where the core shows in accordance response with still and steady raising sea level (Figure 4.4). Northgrippian age is recorded for the high sea level stand from the various land marine interactions (Figure 4.4). One of the reasons cited for this increase in sedimentation is the role of tectonic activity where the area is known for its seismic activity. The sedimentological studies showed coarsening upward sequence during this period that is followed by abrupt shift towards fining up sequence. This appears to be on account of increasing energy due to shallowing of the basin due to earlier high to very high sedimentation rate. During deposition of these sediments, the depositional environment might have transitioned into sub-tidal settings as seen in other coastal settings (Rao and Wagle, 1997, Juyal et al., 2006). The core section shows slight change from fining up to coarsening up sequence with sand-mud couplets of greyish coloured sediments. This coarsening upward sequence in sheltered (non-open coast settings) is not prominent yet points towards the change in environment from sub-tidal to mixed mud flat environment (Alexander et al., 1991; Avramidis et al. 2013). The zone also marks the transgression to regression shift of the sea.

### **Meghalayan Stage/ Late Holocene Stage**

The abrupt change in the sedimentation rate is noted from this period where the sedimentation rates mark the lowest of 0.09 cm/year from the entire core which marked the zone 3 and was suggested to be completely deposited under a regressing sea level

(Figure 4.4). On the global prospect some of the setting shows standstill during this period and few authors reported the withdrawal of the sea due to change in the global sea level. This can also be noted from our core in this particular zone where the change in colour demarcates the first signatures of reducing marine water column at the Banni core site ~4 ka probably due to filling up of the basin of tectonic upliftment (Maurya et al., 2012; Khonde, 2014). This is followed the abrupt change in light to dark coloured coarser sediments in top 5 m of the section that marks the regressive phase and oxidising environment. This upper part of the core section also contains significant salt grains (evaporites) indicating that the marine withdrawal from this region has turned this region in supra-tidal environment prior to reaching its current state when there is no influence of the tidal regimes (Figure 4.4).